The Neurodynamic Decision Variable in Human Multi-Alternative Perceptual Choice

Carmen Kohl [1,2,*], Laure Spieser [1,2], Bettina Forster [2], Sven Bestmann [3], Kielan Yarrow [2]

[1] These authors contributed equally

[2] Department of Psychology, Cognitive Neuroscience Research Unit,

City, University of London, UK

[3] Sobell Department of Motor Neuroscience and Movement Disorders, UCL Institute of Neurology, University College London, UK

* Correspondence: Carmen Kohl

City, University of London

Northampton Square

London

EC1V 0HB

+44 (0)20 7040 8530

carmen.kohl@city.ac.uk

Funding: This work was supported by a Leverhulme Trust Research Project Grant (RPG-2014188).

Declaration of Interests: The authors declare no competing interests.

Abstract

The neural dynamics underpinning binary perceptual decisions and their transformation into actions are well studied, but real-world decisions typically offer more than two response alternatives. How does decision-related evidence accumulation dynamically influence multiple action representations in humans? The heightened conservatism required in multiple compared to binary choice scenarios suggests a mechanism which compensates for increased uncertainty when multiple choices are present by supressing baseline activity. Here, we tracked action representations using corticospinal excitability during four and two-choice perceptual decisions, and modelled them using a sequential sampling framework. We found that the predictions made by leaky competing accumulator models in order to accommodate multiple choices (i.e. reduced baseline activity to compensate increased uncertainty) were borne out by dynamic changes in human action representations. This suggests a direct and continuous influence of interacting evidence accumulators, each favouring a different decision alternative, on downstream corticospinal excitability during complex choice.

Keywords: accumulator model, Hicks' law, leaky competing accumulator, motor evoked potentials, multi-alternative decision-making

Making the right decision quickly is a fundamental evolutionary objective, because being slow, or being wrong, can be fatal. Most real-world decisions offer several possible responses. Given the existence of capacity limitations and joint speed and accuracy constraints, how do humans adapt as the complexity of a decision scenario increases? Hick's law (Hick, 1952) illustrates how the number of choice alternatives can profoundly affect the speed of response, but the neurocognitive basis of this effect has only recently begun to be elucidated (Churchland & Ditterich, 2012).

Many researchers now agree that to make a decision, sensory evidence from the environment is accumulated over time until it becomes sufficient to trigger a response. This process has been formalised in models involving sequential sampling (Brown & Heathcote, 2008; Forstmann, Ratcliff, & Wagenmakers, 2016; Ratcliff & McKoon, 2008; Smith & Ratcliff, 2004; Usher & McClelland, 2001; but see Thura, Beauregard-Racine, Fradet, & Cisek, 2012; Thura & Cisek, 2016). Such models make the putative mechanisms underlying changes in behaviour more concrete. For example, the increased reaction time found when response alternatives proliferate might result from a change in either the quantity of evidence required to reach a decision, or the rate at which information accumulates. Behavioural assays help distinguish these accounts, and some models, including the physiologically plausible leaky competing accumulator (LCA) model (Usher & McClelland, 2001) can account for multi-alternative decision-making in various settings (Bogacz, Usher, Zhang, & McClelland, 2007; Brown, Steyvers, & Wagenmakers, 2009; Ditterich, 2010; McMillen & Holmes, 2006; Tsetsos, Usher, & Chater, 2010; Tsetsos, Usher, & McClelland, 2011). However, only by marrying the quantitative precision of sequential sampling models with appropriate neurodynamic signals can a biologically compelling description of complex choice behaviour emerge.

Much of the neural evidence supporting sequential sampling models comes from experiments using binary choices. For example, single-cell recording in monkeys, a method with sufficient temporal resolution to track the decision variable, has shown that firing rates of neurons in the lateral intraparietal area (LIP), but also the frontal eye field (FEF), and the superior colliculus (SC) display accumulation-to-bound characteristics in two-choice saccadic tasks (Gold & Shadlen, 2000, 2003; Hanks & Summerfield, 2017; Paré & Wurtz, 2001; Roitman & Shadlen, 2002; Shadlen & Newsome,

2001). In humans, a number of electroencephalographic (EEG) signals have been suggested to reflect the decision variable, but only in the context of binary decisions (Donner, Siegel, Fries, & Engel, 2009; O'Connell, Dockree, & Kelly, 2012; Siegel, Engel, & Donner, 2011).

Despite the prevalence of the two-choice task in research settings, some studies have also investigated the neural dynamics of *multi-alternative* decision-making, at least in non-human primates. Seminal work by Basso and Wurtz (1997, 1998) showed that activity of monkey SC neurons decreased with increased possible targets in a saccadic multi-target task. This finding was explored more thoroughly and in the context of sequential sampling models by Churchland, Kiani, and Shadlen (2008) who presented two monkeys with both two and four-choice random dot motion displays. Both kinds of decision showed the same stereotyped levels of LIP activity at the time of response. However, firing rates differed at the beginning of the decision-making process, as four-choice decisions showed reduced firing rates. In sequential sampling models such as the LCA, lower activity in a given accumulator at the beginning of the decision necessitates larger excursions, i.e., more evidence will be required to reach a response boundary. Such heightened conservatism in multiple compared to binary choice scenarios can be interpreted as a mechanism which compensates for increased uncertainty.

Decreased baseline activity has since been supported by a number of single-cell recording studies (Balan, Oristaglio, Schneider, & Gottlieb, 2008; Cohen, Heitz, Woodman, & Schall, 2009; Lee & Keller, 2008). Does this result generalise to humans and/or different sensorimotor pathways? Given that other plausible mechanisms accounting for changes in behaviour with the number of choice alternatives can be formulated, via either sequential sampling models (e.g. changes in the rate of evidence accumulation) or alternative perspectives (e.g. Hick's original information-theoretic account) this question holds theoretical importance. However, we are not aware of any studies which have directly investigated dynamic neural correlates of binary vs. multi-choice evidence accumulation in the human brain.

Here, we address this longstanding question by assessing the impact of multiple alternatives on the neurodynamic decision variable in humans. Since high temporal resolution data is a prerequisite to tackle this issue, and motor-related EEG/MEG signals have limited utility for decisions with more than

two response alternatives, we use transcranial magnetic stimulation (TMS) for this purpose[1]. TMS motor evoked potentials (MEPs) can be used to read-out decision-related influences in the primary motor cortex or adjacent premotor areas (Bestmann et al., 2008; Bestmann & Krakauer, 2015; Hadar, Makris, & Yarrow, 2012; Hadar, Rowe, Di Costa, Jones, & Yarrow, 2016; Kiers, Fernando, & Tomkins, 1997). When a decision requires an immediate motor response, motor preparation occurs continuously throughout the decision-making process (de Lange, Rahnev, Donner, & Lau, 2013; Duque, Lew, Mazzocchio, Olivier, & Ivry, 2010; Gluth, Rieskamp, & Büchel, 2013; Hadar et al., 2012; Michelet, Duncan, & Cisek, 2010; Tsetsos, Pfeffer, Jentgens, & Donner, 2015; Thura & Cisek, 2016). Therefore, the corticospinal excitability that MEPs reflect can be used as a correlate of the decision variable, and compared directly to the predictions of accumulator models such as the LCA.

By mapping two separate responses, each recruiting a different muscle, to each hand and measuring the activity of both muscles in the hand contralateral to brain stimulation, we were able to record MEPs associated with each response separately. Although single-cell recording studies of decision-making (e.g. Basso & Wurtz, 1997, 1998; Churchland et al., 2008) have typically targeted regions that are anatomically remote from those interrogated using MEPs, their functional roles for the generation of saccades may mirror those of the corticospinal tract for manual actions. We therefore hypothesised that if changes in corticospinal excitability are driven by accumulation-to-bound dynamics as encapsulated in the LCA model, MEP changes associated with each response would display typical characteristics of a decision variable. Specifically, we expected the MEPs' build-up rate to increase with evidence strength, and their amplitudes to reach a stereotyped level at the time of response (Hadar et al., 2016; Spieser, Kohl, Forster, Bestmann & Yarrow, 2018). Importantly, beyond these typical accumulation-to-bound dynamics, we also predicted a reduced amplitude (for potential responses) when participants prepared a four-choice compared to a two-choice decision, as suggested by previously observed lower baseline neural firing rates in non-human primates. Note that this was in no sense inevitable, as there are fundamental differences between single-cell recordings of oculomotor

[1] Other physiological signals may also be appropriate for this purpose, for example EMG (Servant, White, Montagnini, & Burle, 2015, 2016) or the gain of reflex responses (Selen, Shadlen, & Wolpert, 2012). Our choice in part reflects our relative expertise with these techniques, but also the greater likelihood that action-related signals are contaminated by factors unrelated to decision formation as we move further along the sensorimotor pipeline towards the observable action.

neurons in monkeys and the MEP signals reported here. For example, while simultaneous movements of both hands are possible, the oculomotor system is restricted to a movement in a single direction at any given time, which may lead to differences in decision-related neural dynamics. In addressing the possible generalisation of this result from the monkey oculomotor system to the human corticospinal tract, we were able, for the first time, to track the decision variable during human multi-alternative decision-making. We thus distinguish theoretical accounts of Hick's law at a neurocognitive level, by demonstrating decreased levels of baseline activity with an increased number of alternatives.

Methods

Participants

We recruited 13 participants (five males) with a mean age of 26.23 (*SD* = 7.67). Because many TMS trials must be discarded for unavoidable reasons (see EMG Processing below; c.f. Hadar et al., 2016) each participant completed between two and four sessions (each lasting 1-3 hours) and completed on average 4166 trials. Participants were paid £8 per hour. All procedures were approved by the City, University of London Psychology Department Ethics Committee.

Stimuli, Design and Procedure

Participants completed a colour-discrimination task. In each trial, an array of coloured pixels appeared. Arrays consisted of four different colours (green (RGB [0 0.6 0]), red (RGB [0.8 0 0]), yellow (RGB [0.92 0.74 0]), blue (RGB [0.12 0.12 0.61])). Participants were instructed to indicate which colour was most prevalent as quickly and as accurately as possible, using the corresponding one of four response buttons (see Figure 1).

Stimuli were generated using Matlab (The Mathworks, Natick, U.S.A.) and the Psychtoolbox extension (Brainard, 1997; Kleiner et al., 2007; Pelli, 1997), and presented on a Display++ LCD monitor (Cambridge Research Systems, Ltd., Rochester, UK, display size: 41 cm x 30 cm) operating at a refresh rate of 100 Hz and a resolution of 1240 x 786 pixels. Participants sat approximately 100 cm from the screen. The stimulus array subtended 6 x 6 degrees of visual angle. Each coloured pixel spanned 2 x 2 screen pixels, resulting in an array of 145 x 145 coloured pixels.

Participants held two digital response buttons interfaced via a 16 bit A/D card (National Instruments X-series PCIe-6323, sampling rate 100,000 Hz) in each hand, one between thumb and index finger (pinch), and one against the palm, attached to a plastic cylinder (grasp; Hadar et al., 2012). Pinching contracted the first dorsal interosseous (FDI) muscle, while grasping the cylinder activated the abductor digiti minimi (ADM) muscle. Each colour was mapped to one of the four response buttons. The colour-response mapping was randomised across participants.

Trials consisted of a cue (500 ms), a coloured stimulus array (2000 ms or until response), and an inter-stimulus interval (minimum 500 ms). The experiment contained both two and four-choice trials. Additionally, as a positive control, we crossed a manipulation of difficulty with our manipulation of number of choices in a 2x2 design. Difficulty negatively affects accumulation rate (Mulder, van Maanen, & Forstmann, 2014; Ratcliff & Rouder, 1998; Teodorescu & Usher, 2013) and this effect has been demonstrated in MEP signals for two-choice tasks (Hadar et al., 2016; Spieser et al., 2018). To manipulate task difficulty, the percentage of pixels of the dominant colour varied between 33% (easy) and 30% (hard). The remaining colours each took up 22% and 23% of the array respectively. The cue at the beginning of each trial informed participants whether a given trial was a two or a four-choice trial by presenting either two or four coloured squares representing the possible choices.

One third of trials were four-choice, one third were two-choice ‘within’ hands, i.e. the two possible responses were on one hand (left pinch - left grasp, right pinch - right grasp), and one third of trials were two-choice ‘between’ hands, i.e. homologous responses from both hands were possible (left pinch - right pinch, left grasp - right grasp). Trial order was randomised. Note that the difference between two and four-choice trials lay solely in the instructions conveyed by the cue – the stimulus array and the percentage of the four colours did not change. In the first session, participants completed 150 practice trials, to familiarise themselves with the task. Participants then completed between five and six experimental blocks per session, with each block consisting of 168 trials (plus additional trials to regulate TMS frequency; see below).

Stimulation and Recording

Muscle activity was recorded using surface electromyography (EMG), sampled at 1000 Hz via a 13 bit A/D Biometrics Datalink system (version 7.5, Biometrics Ltd., Ladysmith, VA, U.S.A., 2008) and band-pass filtered (20 to 450 Hz). Surface Ag/AgCl electrodes (22 mm x 28 mm, part No. SX230FW, Biometrics Ltd., Ladysmith, VA) were placed above the first dorsal interosseous (FDI) and abductor digiti minimi (ADM) of each hand. Reference electrodes were placed approximately 2 cm from each of the four active electrodes. The EMG signals of the right ADM and FDI were also passed to speakers placed on the left and right of the participant respectively, with noise informing participants that their muscles were not fully relaxed between responses.

Single-pulse TMS was applied using a Magstim Rapid^2 biphasic stimulator (The Magstim Co. Ltd., Whitland, UK). To induce motor evoked potentials (MEP) in both the ADM and the FDI of the right hand, a 70-mm figure-of-eight coil (external casing diameter approximately 90 mm for each loop) was positioned on the scalp over the left motor cortex. The exact location and stimulation intensity was adjusted for each participant individually and set at approximately 110% of the resting motor threshold (RMT). The RMT was defined as the minimal intensity to elicit an MEP with a peak-to-peak amplitude of approximately 50 μV in 50% of stimulations on both the FDI and ADM of the right hand. TMS position was continuously tracked and maintained using a neuro-navigation system (Visor 2, ANT Neuro, The Netherlands).

TMS pulses were planned in 57% of trials from each condition. To ensure a good distribution of TMS pulses during a baseline interval and over the course of the reaction time, TMS trials were divided into four equally frequent time bins between -200 and 700 ms relative to the stimulus onset (i.e. between 300 and 1200 ms relative to cue onset). Within a given bin, the exact stimulation time was drawn randomly for each trial. Since the experiment followed a single-pulse TMS protocol, pulses were required to occur at a maximal frequency of 0.2 Hz. If, by chance, a planned inter-pulse interval (IPI) was less than 5000 ms, timing was adjusted. For IPIs of 4-5000 ms, the inter-trial interval was increased, decreasing the pulse frequency to 0.2 Hz. For IPIs less than 4000 ms, the planned trial was replaced with the next planned stimulation-free trial. If there were no stimulation-free trials left,

random stimulation-free trials were generated in order to increase the IPI. On average, this method added 434 trials per session, yielding an average 1354 trials per session. Planned pulses were not delivered if a response had already been detected.

EMG Processing

Pre-processing: All EMG processing was performed in Matlab (The Mathworks, Natick, U.S.A.). To remove potential differences in movement time (between right and left hands, or pinch and grasp responses), analyses were conducted based on EMG RTs, i.e., the time between stimulus and responding EMG onset. First, the Teager-Kaiser energy operator (TKEO) was applied to detect the onset time of muscle activity associated with each response (Li & Aruin, 2005; Li, Zhou, & Aruin, 2007; Solnik, Rider, Steinweg, Devita, & Hortobágyi, 2010). The discrete TKEO ψ for a given EMG value x of the sample n was defined as:

$$\psi[x(n)] = x^2(n) - x(n+1)x(n-1) \quad (1)$$

A threshold (T) identified the onset of muscle activity:

$$T = \mu + h\sigma \quad (2)$$

With μ and σ representing the baseline mean and standard deviation (-300 to 200 ms relative to cue onset), and h set to 3. Additionally, all trials were visually inspected and the EMG onset time was adjusted manually if necessary. Visual inspection provided no information about the experimental condition of a given trial. Trials with muscular artifacts, no detectable EMG onset, or partial responses on more than one channel were excluded (6.41% of all recorded trials). We further excluded trials with button RTs of ≥ 2000 ms or ≤ 180 ms, or EMG RTs of ≥ 1850 ms or ≤ 30 ms (< 1% of all recorded trials).

In TMS trials, MEP amplitudes in both channels (FDI and ADM) of the right hand were defined as the maximum minus the minimum EMG value from 10-40 ms after stimulation. Trials with muscular pre-activation (EMG > 50 μV in the 200 ms period preceding stimulation) were excluded (4.51% of all trials), as were trials with no visible MEP or in which MEP amplitude was uncertain due to amplifier saturation (2.02% of all trials). Trials were also excluded if the participant's response preceded the planned TMS (4.36% of all trials).

In total, 17.53% of all recorded trials (including 35.38% of TMS trials) were discarded, with a similar proportion of trials deleted across conditions. After these pre-processing steps 44,669 usable trials remained (including 13,588 TMS trials). MEP amplitudes were then z-scored per muscle, session, and participant (but regardless of experimental condition), to normalise their magnitudes. Finally, for all analyses except our baseline comparison (see below), MEPs amplitude associated with incorrect trials were discarded, leading to a total of 11,590 remaining TMS trials.

Re-categorisation: The FDI and ADM channels were reclassified into one of four categories. MEPs from muscles associated with the correct response were classed as 'Correct', while MEPs from the non-responding muscles formed three different error categories, 'Adjacent Error 1', 'Adjacent Error 2', and 'Opposite Error'. Note that for MEP data, these labels generally refer to all potential responses within a given decision, not overt errors (i.e. 'Opposite Error' refers to a response which would be incorrect, had it been made). Figure 1 illustrates these mappings. The response opposite to the 'Correct' response, corresponding to the non-homologous movement on the incorrect hand, was labelled 'Opposite Error'. We used 'Adjacent Error 1' for responses which were incorrect but on the correct hand in four-choice trials, or responses which were cued but incorrect in two-choice trials. The remaining responses were labelled 'Adjacent Error 2'. Note however, that stimulation provided only two (right-hand) MEPs per trial which were sorted into two of the four categories.

Collation and Smoothing: For each correct/error category and each condition, MEPs recorded in correct trials were pooled across participants and sessions. We therefore normalised stimulation times for each session and participant, expressing them as a percentage of median EMG RT (on stimulation-free trials). Pooled MEP amplitudes were sorted in time and aligned to both the stimulus and the response.

To generate continuous signals, MEP amplitudes were then smoothed via a Gaussian kernel:

$$\widehat{Y}(t) = \frac{\sum_{i=1}^{N} e^{\left(-\frac{(t-t_i)^2}{2\sigma^2}\right)} Y_i}{\sum_{i=1}^{N} e^{\left(-\frac{(t-t_i)^2}{2\sigma^2}\right)}} \quad (3)$$

Where N is the number of MEPs, each being associated with a magnitude Y_i and a time t_i. The smoothed signal was calculated in time steps of 1% median EMG RT, using a smoothing kernel with a full-width half maximum of 5% median EMG RT.

Statistical Analysis: We report two-tailed p values for all pairwise tests. Differences between conditions for behavioural data (i.e. RTs, EMG RTs and errors) were inferred using ANOVAs and generalized linear mixed models (GLMMs) with logistic link functions, respectively. GLMMs were implemented using the Matlab fitglme command, and all effects of interest (e.g. difficulty, number of response alternatives and their interaction) were nested within participants and sessions and included as random effects in the model specifications.

For TMS data, based on previous research in non-human primates (Balan et al., 2008; Churchland et al., 2008; Cohen et al., 2009), we expected reduced baseline MEP amplitudes when participants chose between four compared to two alternatives. To test this, we took (for each participant) the amplitude of all z-scored MEPs recorded during the cue-stimulus interval and associated with a cued response (i.e., for four-choice trials, all MEPs during the baseline-period, while for two-choice trials, only MEPs categorised as 'Correct' or 'Adjacent Error 1'). Following translation and square-root transformation of these scores to achieve normality, the difference across conditions was tested using a linear mixed model (with random effects for participant) using the Matlab fitlme command (which, when compared to a traditional t-test performed on averages derived from multiple trials, better utilises information from all contributing scores). This approach was also applied to an unforeseen prediction emerging from our modelling, regarding differences in late accumulation profiles between opposite errors and other (i.e. adjacent) categories of error.

We also expected the MEP signal to be affected by task difficulty, with steeper accumulation for 'easy' than 'hard' trials. Under sequential sampling models with multiple accumulators, the *difference* in their accumulation rates is a key determinant of behaviour. Hence we focussed on trials in which two MEPs from a single hand could be used to construct a signal measuring the difference between 'Correct' and 'Adjacent Error 1' responses, a signal which has previously been shown to display differences between difficulty conditions (Hadar et al., 2016). For both four-choice and two-

choice-within-hand trials, we fitted a straight line to the MEP signals derived from this difference. We term the gradient of this line a relativized slope. We did this for both 'easy' and 'hard' trials, then subtracted the relativized slope for 'hard' trials from the slope associated with 'easy' trials. These estimates were made for stimulus-locked data, between 50% and 90% median EMG RT, and response-locked data, between -50% and -10% median EMG RT. We used non-parametric permutation tests with 1999 iterations to generate new sets of resampled 'easy' and 'hard' conditions (without replacement) and calculated the relativized slope difference between them. In each test, the original difference was compared to the resulting null distribution of differences. Note that because these permutation tests were performed on a collated set of trials from all participants, the statistical generalisation is to a sampling distribution based on all possible trials from our *particular* set of participants, rather than one based on all possible participants.

Modelling

We used the LCA model to fit the behavioural data (Usher & McClelland, 2001). The LCA is a race accumulator model and therefore easily extended to more than two alternatives. Accumulation traces are defined by an accumulation rate *v* plus noise, and race towards a decision boundary *A*. The LCA is designed to explain the accumulation process in a more neurophysiologically plausible way than other models within this framework. To this end, it includes a leakage parameter *k* as well as a parameter β for mutual inhibition between accumulators. Thus, in a binary decision involving the accumulators *m* and *n*, the change in activation in accumulator *m* is given by:

$$dx_m \propto v_m - kx_m - \beta x_n + N(0, \sigma^2) \quad (4)$$

Where *v* is the input into the accumulator and $N(0,\sigma^2)$ is normally distributed noise with zero mean and a standard deviation σ. Additionally, the accumulation process is forced to remain positive:

$$x_m(t+1) = \max(0, x_m(t) + dx_m) \quad (5)$$

RT is made up of the time required to reach the boundary *A*, and a non-decision time T_{er}, which accounts for sensory and motor processes before and after the decision process.

Model Fit: We tested three LCA models (see Table 1). In Model 1, we extended the model to include four accumulators. In a four-choice trial, the accumulation rate of the correct accumulator was given by $v_{correct}$, while accumulation rate for all other accumulators was given by $v_{incorrect}$. The starting point $z_{four\text{-}choice}$ was set to 0, and along with the threshold A and the leakage k, equal across accumulators. Two parameters, β_{adj} and β_{opp}, captured inhibition between accumulators. Inhibition parameters reflected the anatomical adjacency of responses. Specifically, β_{opp} describes the inhibition induced by the evidence associated with the opposite response and opposite hand relative to a given accumulator, while inhibition between all other accumulators is given by β_{adj} (see Figure 2). This means that the change in accumulation for each accumulator is given by:

$$dx_{Correct} \propto v_{Correct} - kx_{Correct} - \beta_{adj}x_{Adj.Err1} - \beta_{adj}x_{Adj.Err2} - \beta_{opp}x_{Opp.Err} + N(0,\sigma^2)$$

$$dx_{Adj.Err1} \propto v_{Adj.Err1} - kx_{Adj.Err1} - \beta_{adj}x_{Correct} - \beta_{adj}x_{Opp.Err} - \beta_{opp}x_{Adj.Err2} + N(0,\sigma^2)$$

$$dx_{Adj.Err2} \propto v_{Adj.Err2} - kx_{Adj.Err2} - \beta_{adj}x_{Correct} - \beta_{adj}x_{Opp.Err} - \beta_{opp}x_{Adj.Err1} + N(0,\sigma^2)$$

$$dx_{Opp.Err3} \propto v_{Opp.Err} - kx_{Opp.Err} - \beta_{adj}x_{Adj.Err1} - \beta_{adj}x_{Adj.Err2} - \beta_{opp}x_{Correct} + N(0,\sigma^2)$$

(6)

In two-choice decisions the same four-accumulator structure was used with the following exceptions. Based on previously demonstrated baseline differences (e.g. Churchland et al., 2008), accumulators associated with the cued responses ('Correct' and 'Adjacent Error 1') began at a starting point defined by $z_{two\text{-}choice\text{-}cued}$, while the starting point of the other two accumulators ('Adjacent Error 2' and 'Opposite Error') $z_{two\text{-}choice\text{-}uncued}$ was set to 0. The accumulation rate of the two accumulators associated with the non-cued responses ('Adjacent Error 2' and 'Opposite Error'), was also set to 0, so that only noise was accumulated.

Lastly, the drift rates $v_{corrrect}$ and $v_{incorrect}$ varied across difficulty levels, yielding in total 10 free parameters ($v_{easy\text{-}correct}$, $v_{easy\text{-}incorrect}$, $v_{hard\text{-}correct}$, $v_{hard\text{-}incorrect}$, $z_{two\text{-}choice\text{-}cued}$, k, β_{adj}, β_{opp}, σ^2, T_{er}). The boundary parameter A was set to 1 as a scaling parameter. Model 1 is schematized in Figure 2.

By setting the accumulation rate of the non-cued accumulators to 0 in Model 1, we assumed early attentional selection, gating the signal at a sensory level. Since this is speculative, we also tested a model without this assumption. Model 2 is identical to Model 1, except that accumulation rates of

uncued accumulators in two-choice conditions ('Adjacent Error 2' and 'Opposite Error') were not set to 0, but instead to the same $v_{incorrect}$ as 'Adjacent Error 1'. Hence this model had the same 10 free parameters as Model 1.

Finally, we also tested a model with no baseline difference between two-choice and four-choice conditions, but which introduced a difference in accumulation rate instead. Hence Model 3 is identical to Model 1 with the exception that the starting point is set to 0 for all conditions, and that two-choice and four-choice conditions have separate correct and incorrect drift rates ($v_{easy\text{-}four\text{-}correct}$, $v_{easy\text{-}four\text{-}incorrect}$, $v_{easy\text{-}two\text{-}correct}$, $v_{easy\text{-}two\text{-}incorrect}$, $v_{hard\text{-}four\text{-}correct}$, $v_{hard\text{-}four\text{-}incorrect}$, $v_{hard\text{-}two\text{-}correct}$, $v_{hard\text{-}two\text{-}incorrect}$). Like Model 1, accumulation rates in uncued accumulators were set to 0. This resulted in a total of 13 free parameters for Model 3 ($v_{easy\text{-}four\text{-}correct}$, $v_{easy\text{-}four\text{-}incorrect}$, $v_{easy\text{-}two\text{-}correct}$, $v_{easy\text{-}two\text{-}incorrect}$, $v_{hard\text{-}four\text{-}correct}$, $v_{hard\text{-}four\text{-}incorrect}$, $v_{hard\text{-}two\text{-}correct}$, $v_{hard\text{-}two\text{-}incorrect}$, k, β_{adj}, β_{opp}, σ^2, T_{er}).

Note that we did not test a model with varying decision boundaries, a variation which is commonly used (e.g. Brown & Heathcote, 2008). In fact, sequential sampling models are unable to distinguish between variations in starting points, variations in boundaries, or a combination of both based on model fits alone (Bogacz, Wagenmakers, Forstmann, & Nieuwenhuis, 2010). Hence we tested only one of these accounts and, in accordance with suggestions made in the literature (Balan et al., 2008; Basso & Wurtz, 1997, 1998; Churchland et al., 2008), chose a variation in baseline (Model 1/2) to model differences in accumulation excursion between binary and multiple choice alternatives.

To fit each model, normalised EMG RTs from stimulation-free trials were pooled across participants to estimate the model parameters at the group level. A total of 20,000 simulated EMG RTs were compared to the empirical data using Quantile Maximum Probability Estimation (Heathcote, Brown, & Mewhort, 2002) and parameter values were adjusted using a differential evolution algorithm implemented in Matlab (The Mathworks, Natick, U.S.A.; Price et al., 2005).

The three models were compared by calculating two measures of goodness-of-fit which consider both likelihood and the number of free parameters, namely the Bayesian information criterion (BIC, Schwarz, 1978) and the Akaike information criterion (AIC; Akaike, 1977). The best fitting model by these measures was then used to generate predicted accumulation profiles.

Predicted Neurodynamics: We simulated 20,000 accumulation paths for each condition, based on best-fitting parameter values obtained for the model showing the best goodness-of-fit to behavioural data. Since we fitted using EMG RTs rather than button RTs (i.e. time to move effectors was not included) we assumed that virtually all of the estimated non-decision time described sensory processes. We therefore started the accumulation profile after a sensory delay given by T_{er}.

MEPs were simulated as the amplitude of a given accumulator at random MEP latencies. Just as in the experimental data, only simulated MEPs that occurred before the decision boundary was reached were retained. The timing of simulated MEPs associated with correct decisions was then expressed relative to both stimulus and response, and MEPs were smoothed to create simulated continuous MEP signals.

Results

We explored multi-alternative decision-making in humans by utilising MEP signals as a correlate of the decision variable. Since we were a priori uncertain about how anatomical proximity of responses would affect decision-making, our design initially distinguished two sub-conditions of two-choice trials, depending on whether cued responses were contained within or spread between hands (Figure 1 b). However, since we found no behavioural or neural evidence to suggest that they should be treated separately, we pooled two-choice data for most of our analyses.

Our approach tracked the evolution of preparation for each of up to four response alternatives, which we categorised as ‘Correct’, ‘Adjacent Error 1’, ‘Adjacent Error 2’, and ‘Opposite Error’ (see Methods and Figure 1). We used an LCA model with four accumulators categorised in the same way to model behavioural data and predict the accumulation profile of each accumulator. We were thus able not only to describe neurodynamic decision variables with four or two response alternatives, but also to directly compare their profiles to model predictions.

Behaviour for two-choice and four-choice decisions follows Hick's law and reflects choice difficulty

Since the application of TMS pulses can alter response times (Day et al., 1989), only stimulation-free trials remaining after pre-processing of electromyography (EMG) were used for behavioural analyses. Figure 3 shows mean behavioural results obtained in each condition. For these analyses, which did not rely on pooling of data across participants (unlike subsequent analyses of the decision variable), we report raw, non-normalised response times. The effects of 'Number of Alternatives' and 'Difficulty' on correct EMG RT were tested with a 2x2 repeated-measures ANOVA. EMG RTs were longer for decisions with four alternatives than decisions with two alternatives, $F(1, 12) = 207.10$, $p < .001$, $\eta_p^2 = .95$. Also, harder decisions were slower than easy ones, $F(1, 12) = 117.37$, $p < .001$, $\eta_p^2 = .91$. There was no significant interaction between the two factors ($p = .68$). The same analysis with button RT as time of response led to qualitatively identical results (main effect of 'Number of Alternatives': $p < .001$, main effect of 'Difficulty': $p < .001$, interaction effect: $p = .76$). These results are consistent with Hick's law.

Error data are known to violate the assumptions of ANOVA. We therefore instead applied generalised linear mixed-effects models for statistical inference, which revealed significantly lower accuracy in four-choice compared to two-choice trials, $t(156) = 5.59$, $p < .001$, and in hard compared to easy trials, $t(156) = 9.68$, $p < .001$, with no interaction ($p = .052$). These results demonstrate that our RT findings do not represent a speed/accuracy tradeoff: Participants were both slower and less accurate in four-choice (and hard) trials. Additionally, we compared the proportions of errors arising in the different possible erroneous response categories (Figure 3 b). In two-choice trials, the three categories differed significantly from each other, $t(117) > 2.58$, $p < .01$, with most errors in the 'Adjacent Error 1' category, and least 'Opposite' errors. In four-choice trials, 'Opposite' errors were less frequent, although only 'Adjacent Error 1' and 'Opposite Error' categories differed significantly, $t(117) = 2.27$, $p = .03$. These results indicate that both of the cued responses were prioritised in two-choice trials, and that task-irrelevant anatomical constraints affected action selection in our experiment.

Corticospinal excitability reflects the accumulation of evidence and is reduced at baseline with four compared to two choices

When analysing corticospinal excitability, we generally focused on trials in which the correct response was ultimately executed (as we had insufficient overt error trials to yield reliable signals). Smoothed signals were generated using MEPs from muscles associated with each potential response category. The resulting signals are displayed in Figure 4, locked to both the stimulus (upper panels) and the response (lower panels). Following an initial ubiquitous negative drift, in each condition corticospinal excitability associated with the correct response increased as expected over the course of the decision to reach a higher magnitude than all other potential responses, while the 'Opposite Error' response showed the lowest amplitude.

Contrary to our expectations, there was little difference between 'easy' (solid lines) and 'hard' (dashed lines) trials in any of the conditions. There were, however, marked differences between four-choice and two-choice decisions. In the four-choice condition, 'Adjacent Error 1' (same hand but different action relative to the responding muscle) and 'Adjacent Error 2' (other hand but homologous action) traces followed a virtually identical profile of corticospinal excitability. In two-choice trials on the other hand, the two cued responses ('Correct' and 'Adjacent Error 1') are separated from the uncued response traces ('Adjacent Error 2' and 'Opposite Error') throughout the beginning of the trial (note that the cue onset is prior to the onset of MEP recording). Only towards the end of the decision, presumably when the (time-lagged) process driving selection of the correct response begins to feed continuously into motor cortex, does the 'Correct' response increase at a steeper rate relative to the 'Adjacent Error 1' response.

To test our hypothesis predicting lower baseline activity in four compared to (cued) two-choice decisions, we compared MEP amplitudes during the cue-stimulus interval (-200 to 0 ms relative to the stimulus onset; equivalent to 300 to 500 ms relative to cue onset). We applied a linear mixed-effects model, which confirmed our hypothesis, revealing significantly reduced MEP amplitudes in four compared to two-choice trials, $t(5112) = 2.23$, $p = .026$ (see Figure 4).

Additionally, we tested the difference in relativized slopes (i.e. correct minus error accumulation rates) between different difficulty levels (for both four-choice and two-choice-within-hand trials; solid vs. dashed lines in Figure 4) using a permutation procedure (see Methods). This analysis focussed on the final half of the RT period, when differential evidence accumulation between potential responses was observable in corticospinal excitability traces. The empirical slope difference between 'easy' and 'hard' trials did not exceed the upper/lower 2.5% of their bespoke null distributions, for either stimulus-locked or response-locked MEPs, with either four or two choices. Hence, contrary to our prediction and to previous evidence (e.g. Spieser et al., 2018), there was no easy/hard slope difference ($p > .05$). To the extent that MEP signals do appear to diverge between easy and hard conditions (e.g. late on during four-choice trials) this divergence is uninterpretable due to high levels of sampling noise.

However, to further explore this unexpected finding, we compared the difference in relativized slopes between fast and slow responses by performing a median split on the data. We then used the same permutation method previously applied to test the difference in slope between 'easy' and 'hard' trials to instead compare slopes of slow and fast trials. We found that slopes in fast trials were significantly higher than slopes in slow trials (for both four-choice and two-choice-within-hand trials), albeit only in the stimulus-locked signal ($p < .05$), showing that when responses were quicker, corticospinal excitability accumulation was steeper.

Behavioural Modelling suggests a competitive accumulation process in which changes in baseline-to-boundary distance generate Hick's law

To examine whether accumulation-to-bound models can provide a compelling neurocognitive account of Hick's law, we first fitted a sequential sampling model to the behavioural data. Both the overall parameterisation of such a model, selected via model comparison procedures, and the specific changes observed in the resulting parameters across experimental conditions, provide insights into the processes that drive behavioural effects. Here, we used the LCA model (Usher & McClelland, 2001), which lends itself easily to multiple-alternative decision-making.

We fitted three LCA model variants to the EMG RT data, all of which included four accumulators and assumed that accumulation rate varied between easy and hard trials. They also assumed the existence of inhibition between accumulators, defined by two inhibition parameters (based on the anatomical adjacency of responses). Our best-fitting model (Model 1 in Table 1, with 10 free parameters) additionally assumed the same accumulation rate in four and two-choice trials, but a difference in starting point. Hence this model instantiates an account of Hick's law in which baseline-to-boundary distance drives behavioural changes as the number of alternatives increases. For this model, accumulation rates of uncued accumulators in two-choice trials were set to zero.

As seen in Table 1, varying model assumptions in other a priori plausible ways (by assuming either non-gated evidence accumulation in uncued accumulators – Model 2, 10 parameters – or different accumulation rates in four and two-choice trials – Model 3, 13 parameters) did not improve the goodness-of-fit, as indexed by the Bayesian and Akaike information criteria (BIC/AIC). Because these different model variants capture alternative accounts of Hick's law (in particular, for Model 3, a different rate of evidence accumulation generates differences in RT and errors) this suggests that introducing multiple alternatives into a decision-making process primarily affects the baseline-to-boundary distance of the accumulation process, with a lower starting point in four compared to two-choice decisions. We therefore proceeded using Model 1 (schematised in Figure 2), for which parameter estimates are displayed in Table 2. Notice how the starting point of accumulation (parameter z) is higher in two-choice cued conditions compared to other conditions. The best-fitting model also suggests greater inhibition (β) between opposite responses than between adjacent ones, and higher accumulation rates (v) in easy compared to difficult conditions.

The quality of the fit is shown in Figure 5 (left: four-choice; right: two-choice; top: easy; bottom: hard). The observed (circles) and simulated (lines and crosses) normalised EMG RT distributions are summarised by five quantile estimates (from left to right: 10%, 30%, 50%, 70%, 90%), and the EMG RT (x-axis) and proportion of data (y-axis) associated with each quantile are displayed. Both correct responses (thick lines) and responses in each error category are shown, with the latter on a magnified scale for clarity. The overlap between empirical and simulated quantiles indicates

a good overall model fit: The model successfully predicted the complete RT distributions of both correct and erroneous responses. The mean absolute difference between predicted and recorded EMG RT quantiles was approximately 2.5% of median EMG RT for correct responses, confirming that the LCA was able to account for both four and two-choice decisions.

Neurodynamic LCA model predictions capture both expected and unexpected features of corticospinal excitability

To be compelling from a neuroscientific perspective, a model should describe both behaviour and its neural substrate, and be able to account for observed features of data that cannot easily be predicted otherwise. Hence we went on to use the estimated parameters derived from our behavioural modelling to simulate average accumulation profiles for each condition. Figure 4 displays the resulting stimulus-locked (upper panels) and response-locked (lower panels) predictions for each condition and each accumulator. Note, however, that the predictions have not been fitted to the MEP signal data – they depend instead on fits to the behavioural data, with model selection and parameter estimates based only on those data.

Important qualitative similarities emerged between the MEP signals and the model predictions (Figure 4). Like the MEP signals, LCA 'Correct' accumulation profiles increase to dominate all other accumulators over the course of the decision in all conditions, while the 'Opposite Error' accumulator shows the lowest amplitude throughout. Furthermore, in four-choice conditions, the accumulators associated with 'Adjacent Error 1' and 'Adjacent Error 2' display a virtually identical profile, while in two-choice conditions, the cued accumulators ('Correct' and 'Adjacent Error 1') show a higher activation than the uncued accumulators ('Adjacent Error 2' and 'Opposite Error'). Contrary to our initial hypotheses, but in complete agreement with our neural data, there was no clear difference between 'easy' and 'hard' predicted accumulation profiles.

Given this surprising failure to observe differences between easy and hard conditions, we explored how large a difference between conditions is necessary to result in a visible slope difference. We therefore simulated accumulation profiles based on varying differences between easy and hard

accumulation rates. By simultaneously increasing/decreasing the easy/hard accumulation rates respectively by varying percentages, while keeping all other parameters the same, and visually inspecting the resulting accumulation profiles, we found that slope differences between easy and hard accumulation paths became visible when they were around 2.5 times higher than the empirically observed differences. This increased difference in accumulation rates resulted in simulated reaction time differences which were three times as large as those in the original simulation (e.g. in four-choice correct simulations, the original difference between easy and hard trials was .06 median EMG RT, while the increased difference was .20 median EMG RT).

Additionally, modelling suggested an amplitude difference between the accumulators associated with 'Adjacent Error 2' and 'Opposite Error', which was most pronounced towards the end of the accumulation process. Hence this modelling step led us to revisit our neural data with an additional prediction. To quantify this effect in the neural data, we compared MEPs from the last quarter of the EMG RT period, by applying a linear mixed-effects model (see Statistical Analysis). The results confirmed the amplitude difference between 'Adjacent Error 2' and 'Opposite Error' in both four ($t(462) > 4.59$, $p < .001$) and two-choice ($t(881) > 4.089$, $p < .001$) conditions, further illustrating the similarity between predicted accumulation profiles and MEP signals (see Figure 4).

Discussion

Hick's law (Hick, 1952) describes how RT increases with the number of stimulus-response alternatives, and was initially believed to reflect the rate of information transmission in choice scenarios. However, sequential sampling models like the leaky competing accumulator model (Usher & McClelland, 2001), which have recently been extended to account for neurodynamic data, provide a useful interpretative lens through which to pinpoint the neurocognitive mechanisms that generate such behavioural adaptations. Slower responses might arise from a decreased rate of information accrual, or from a requirement for stronger evidence in the face of greater intrinsic uncertainty. In line with the latter suggestion, previous work has demonstrated that more choice alternatives translate into a lower baseline activity for the decision variable in areas such as macaque LIP (Balan et al., 2008; Churchland

et al., 2008). Here we tested the proposal that such decision-related changes in neuronal activity directly influence action representations in the human brain at the level of motor cortex and the spinal cord. To this end, participants completed a colour-discrimination task with either four or two choices, while we tracked the dynamics of corticospinal excitability for all four possible responses. We found that during perceptual decisions, action representations are continuously updated from a baseline level that varies with task demands, as if dynamically shaped by a competitive accumulation process that trades speed for accuracy as uncertainty increases.

Behaviourally, responses were slower and less accurate with four-choices compared to two-choices (Brown et al., 2009; Cohen et al., 2009; Hick, 1952). These findings indicate that although the stimulus did not change, and the manipulation was implemented only by the cue, the four vs two-choice manipulation had a significant impact on participants' decision-making. Additionally, categorizing error responses in two-choice trials revealed that the cued but incorrect response occurred more often than any other error, while in four-choice trials, errors corresponding to responses sharing some anatomical linkage with the correct response were roughly equal in frequency. Hence, the complexity of the choice scenario affected not only overall response times and accuracy, but also the specifics of response selection on incorrect trials.

Because it is difficult to intuit the predictions of complex multi-parameter models, we fitted a sequential sampling model to the behavioural data in order to simulate evidence accumulation profiles and then compare them to recorded MEP signals, choosing the LCA model for this purpose (Usher & McClelland, 2001). The LCA is an extension of a simple race accumulator model, but includes leakage and inhibition parameters to model a more neurophysiologically plausible accumulation. This relatively complex model was chosen because it is easily extended to any number of choice alternatives (Smith & Ratcliff, 2004; Usher & McClelland, 2001), and has been shown to adequately account for multi-alternative decision-making in a number of previous studies (Bogacz et al., 2007; Ditterich, 2010; McMillen & Holmes, 2006; Tsetsos et al., 2010, 2011). In particular, the inhibition between accumulators appears a necessary model characteristic in order to explain the behaviours associated with the three different error categories utilised here (i.e. the occurrence of fewer opposite than adjacent

errors). By incorporating two inhibition parameters, varying the degree of lateral inhibition between responses, the model accounted for behavioural data involving complex anatomical linkages between effectors. Whether the lower value of the inhibition parameter between 'adjacent' responses actually reflects less lateral inhibition, or a stronger co-activation of responses associated to contiguous stimuli, remains to be elucidated. Other models exist with broadly similar architectures (e.g. multi-alternative decision field theory; Roe, Busemeyer, & Townsend, 2001) and are likely to provide similarly plausible accounts of our data.

We tested three different LCA models. Importantly, the best-fitting model utilised a higher starting point in two-choice than four-choice trials. This model outperformed a variant in which Hick's law was instead implemented via changes in the rate of evidence accrual, thereby confirming that RT and accuracy differences between four and two-choice decisions could arise from reduced baseline activity in multi-alternative choices. Note that we did not test a model which varied in decision boundary rather than starting point. Since these two accounts both affect the excursion of accumulation, they lead to mathematically equivalent RT predictions, and could only be distinguished based on neural results. Because previous results (e.g. Churchland et al., 2008) have shown a difference in baseline activity, we focussed on testing that account.

Specifically, our modelling implied that action representations should evolve dynamically from differing baseline levels during decision-making. We assessed this by using TMS to induce MEPs in right-hand muscles at random times throughout the trial. By pooling data across participants and smoothing the resulting data points, we constructed an MEP signal for each response category separately (Hadar et al., 2016; Klein-Flügge & Bestmann, 2012; Klein-Flügge, Nobbs, Pitcher, & Bestmann, 2013). Here, the response categories refer to potential responses within a given correct decision, rather than overt errors (i.e. 'Opposite Error' refers to a response which would have been incorrect, had it been made). In fact, the labour-intensive nature of the MEP signal, as well as high accuracy rates (~ 80%) meant we were unable to generate MEP signals associated with overt errors.

The resulting MEP signal reflects corticospinal excitability and has previously been associated with decision-related evidence accumulation (Hadar et al., 2016; Spieser et al., 2018). Typically, in

humans, neural correlates of decision-making produce a single waveform per decision, reflecting either a difference or sum of the hypothetical underlying accumulators (e.g. de Lange et al., 2013; Donner et al., 2009; Kelly & O'Connell, 2013). However, here, tracking each of the four potential responses allowed us to estimate each of the four associated accumulators and thereby provide a richer insight into the decision process than a single summary signal could provide.

To our knowledge, this is the first description of a temporally precise neural correlate of the decision variable for multi-alternative vs binary decision-making in humans. For comparison, estimated model parameters were used to simulate accumulation profiles under the LCA model. Crucially, the resulting profiles were qualitatively similar to those of the measured MEP signals, despite the fact that they were predicted from categorically distinct (behavioural) data. In line with our hypotheses, we found a significant baseline difference between four and (cued) two-choice corticospinal excitability. Subsequently, the 'Correct' MEP trace increased throughout the trial and peaked at the response, clearly separated from profiles associated with erroneous responses. Although the clear baseline difference suggests that this is the main mechanism driving changes in RT, it is possible that accumulation excursion is additionally enhanced by a subtle boundary variation, which our method, which inevitably yields less usable MEPs and thus less certainty towards the end of the trial, was less well suited to detect.

We also observed a difference in the trajectories of the potential but erroneous responses between four and two-choice decisions, just as our behavioural modelling predicted. There was no observable difference between potential errors made with the same hand and those made with the homologous effector but the wrong hand in four-choice trials, or, in fact, any of the profiles during the first half of the trial. However, there was a clear separation in two-choice trials, where cued responses showed a higher amplitude than uncued responses throughout the trial. This enhanced activation of the erroneous but cued response affected behaviour, specifically the frequencies with which different categories of error were observed. Similarly, in four-choice trials, responses anatomically linked to the correct alternative showed the greatest activation in the second half of the RT period, with a corollary effect on error rates.

The results described so far were broadly as hypothesised (although we did not make a specific a priori hypothesis regarding our different categories of error). However, model predictions also converged with the MEP signal in surprising ways. Contrary to our prediction, both showed little difference between easy and hard accumulation profiles (beyond that attributable to sampling noise). Previous research has shown that manipulations of difficulty typically affect evidence accumulation (Ho et al., 2009; Ratcliff & McKoon, 2008), as well as associated neural signals (Kelly & O'Connell, 2013; Roitman & Shadlen, 2002), including smoothed MEP signals like the ones used here (Hadar et al., 2016; Spieser et al., 2018). Moreover, modelled accumulation rates were free to vary in each difficulty condition, and indeed suggested that RT differences reflected such variation, with higher slopes for easier decisions. However, the difference did not produce distinct predicted accumulation profiles. This surprising result removes a possible objection regarding the putative role of the MEP signal as an accumulation signal, as, counterintuitively, it showed the very pattern predicted by the model. This convergence is likely explained by a relatively weak manipulation of difficultly. Indeed, even though easy decisions were significantly faster, the effect was small (< 50 ms), probably because the dominant colour in the easy condition took up just 33% of the display, compared to 30% in the hard condition. In fact, similar studies which reported marked slope differences between difficulty conditions also reported much larger reaction time differences (around 150 ms), translating into larger differences in accumulation value (Spieser et al., 2018), suggesting that larger differences in evidence strength are needed to detect a visible difference in build-up rate. A post-hoc analysis confirmed that while there was no slope difference between easy and hard waveforms, fast decisions were associated with higher slopes than slow decisions, at least in the stimulus-locked signal, supporting the role of the MEP as a correlate of accumulation.

Our modelling constrained non-cued alternatives in two-choice trials to have an accumulation rate of zero, implying that attentional mechanisms gate the evidence at a sensory level, before accumulation occurs (Wyart, Myers, & Summerfield, 2015). This model assumption, implemented only because it provided the best behavioural fit, was again supported by our MEP results, which displayed little or no activation of non-cued responses in two-choice trials. Note that this was found despite the

fact that each stimulus contained all four colours, and the response options were determined by pre-stimulus cues alone. This finding is in line with previous research demonstrating that a different neural correlate of accumulation, the centroparietal positivity, only displays a build-up if the sensory evidence provided is directly relevant to the decision (O'Connell et al., 2012).

Despite the similarities we have outlined, there were also some marked differences between predicted and recorded accumulation signals. For instance, the slow negative drift visible in all MEP signals (Figure 4) may reflect broad inhibition processes described during action preparation, resulting in MEP suppression in both responding and non-responding muscles (for a review see Duque, Greenhouse, Labruna, & Ivry, 2017). Naturally, such non-selective MEP modulation was not reproduced in the model predictions. Additionally, the neural data seem to suggest not only a higher baseline for cued responses but also a small simultaneous suppression of uncued responses, which may be an interesting addition to the model. A further slight difference between neural dynamics and model predictions (and indeed characteristics commonly associated with accumulation) relates to the reaching of a stereotyped amplitude at the time of response, which, although not directly tested here, is not clearly visible in the neural data.

At least two reasons might underlie these discrepancies. Firstly, a direct comparison of the model prediction to the data is limited by the quality and nature of the MEP signal. While a signal based on *differences* in MEP size between a responding and non-responding muscle is likely to be a relatively true reflection of decision processes underlying response selection, an MEP signal displaying each response separately, as utilised here, will also contain non-specific influences, such as motor-level processes. Secondly, like any model, the LCA can, at best, be an approximation of the true decision-making process. Importantly, sampling models provide a solid theoretical framework to analyse and interpret decision-related neural activity. However, observed dissimilarities at the decision-variable level illustrate how models describe a simplified decision process which does not always relate in a straightforward manner with the underlying neural dynamics (Purcell & Palmeri, 2017).

In summary, we have demonstrated that multi-alternative decision-making in humans can be accounted for by sequential sampling models, and, importantly, that smoothed MEP signals reflecting

corticospinal excitability provide a downstream reflection of the accumulation process. Under a sequential sampling modelling framework, higher RTs with increasing numbers of alternatives can be explained by a greater distance between the starting point of accumulation and the response boundary. This affects the signal-to-noise ratio, because larger baseline-to-bound distances require more evidence to be accumulated (Churchland & Ditterich, 2012; Churchland et al., 2008; Usher & McClelland, 2001). In four-choice decisions, which increase uncertainty relative to two-choice decisions, an increase in the baseline-to-bound distance would compensate for this uncertainty at the expense of reaction time. Here, we have validated this prediction in human decision-making actuated via the corticospinal tract, showing for the first time that the number of choice alternatives in a decision-making task affects the baseline activity of neural accumulation, just as sequential sampling models predict. Furthermore, we have shown that MEP signals can be used to track the evolution of preparation for each of four responses separately, giving insight into each of the four associated accumulators of a sequential sampling model.

References

Akaike, H. (1977). On entropy maximization principle. In P. R. Krishnaiah (Ed.), *Applications of Statistics* (pp. 27–41). Amsterdam.

Balan, P. F., Oristaglio, J., Schneider, D. M., & Gottlieb, J. (2008). Neuronal correlates of the set-size effect in monkey lateral intraparietal area. *PLoS Biology*, *6*, 1443–58.

Basso, M. A., & Wurtz, R. H. (1997). Modulation of neuronal activity by target uncertainty. *Nature*, *389*, 66–69.

Basso, M. A., & Wurtz, R. H. (1998). Modulation of neuronal activity in superior colliculus by changes in target probability. *Journal of Neuroscience*, *18*, 7519–34.

Bestmann, S., Harrison, L. M., Blankenburg, F., Mars, R. B., Haggard, P., Friston, K. J., & Rothwell, J. C. (2008). Influence of Uncertainty and Surprise on Human Corticospinal Excitability during Preparation for Action. *Current Biology*, *18*, 775–80.

Bestmann, S., & Krakauer, J. W. (2015). The uses and interpretations of the motor-evoked potential for

understanding behaviour. *Experimental Brain Research*, *233*, 679–89.

Bogacz, R., Usher, M., Zhang, J., & McClelland, J. L. (2007). Extending a biologically inspired model of choice: multi-alternatives, nonlinearity and value-based multidimensional choice. *Philosophical Transactions of the Royal Society B: Biological Sciences*, *362*, 1655–1670.

Bogacz, R., Wagenmakers, E. J., Forstmann, B. U., & Nieuwenhuis, S. (2010). The neural basis of the speed-accuracy tradeoff. *Trends in Neurosciences*, *33*, 10–16.

Brainard, D. H. (1997). The Psychophysics Toolbox. *Spatial Vision*, *10*, 433–36.

Brown, S. D., & Heathcote, A. (2008). The simplest complete model of choice response time: Linear ballistic accumulation. *Cognitive Psychology*, *57*, 153–78.

Brown, S., Steyvers, M., & Wagenmakers, E. J. (2009). Observing evidence accumulation during multi-alternative decisions. *Journal of Mathematical Psychology*, *53*, 453–62.

Churchland, A. K., & Ditterich, J. (2012). New advances in understanding decisions among multiple alternatives. *Current Opinion in Neurobiology*, *22*, 920–26.

Churchland, A. K., Kiani, R., & Shadlen, M. N. (2008). Decision-making with multiple alternatives. *Nature Neuroscience*, *11*, 693–702.

Cohen, J. Y., Heitz, R. P., Woodman, G. F., & Schall, J. D. (2009). Neural Basis of the Set-Size Effect in Frontal Eye Field: Timing of Attention During Visual Search. *Journal of Neurophysiology*, *101*, 1699–1704.

Day, B. L., Rothwell, J. C., Thompson, P. D., Maertens de Noordhout, A., Nakashima, K., Shannon, K., & Marsden, C. D. (1989). Delay in the execution of voluntary movement by electrical or magnetic brain stimulation in intact man. Evidence for the storage of motor programs in the brain. *Brain*, *112*, 649–63.

de Lange, F. P., Rahnev, D. A., Donner, T. H., & Lau, H. (2013). Prestimulus Oscillatory Activity over Motor Cortex Reflects Perceptual Expectations. *Journal of Neuroscience*, *33*, 1400–10.

Ditterich, J. (2010). A comparison between mechanisms of multi-alternative perceptual decision making: Ability to explain human behavior, predictions for neurophysiology, and relationship with decision theory. *Frontiers in Neuroscience*, *4*, 1–24.

Donner, T. H., Siegel, M., Fries, P., & Engel, A. K. (2009). Buildup of Choice-Predictive Activity in Human Motor Cortex during Perceptual Decision Making. *Current Biology*, *19*, 1581–85.

Duque, J., Greenhouse, I., Labruna, L., & Ivry, R. B. (2017). Physiological Markers of Motor Inhibition during Human Behavior. *Trends in Neurosciences*, *40*, 219–36.

Duque, J., Lew, D., Mazzocchio, R., Olivier, E., & Ivry, R. B. (2010). Evidence for Two Concurrent Inhibitory Mechanisms during Response Preparation. *Journal of Neuroscience*, *30*, 3793–802.

Forstmann, B. U., Ratcliff, R., & Wagenmakers, E.-J. (2016). Sequential Sampling Models in Cognitive Neuroscience: Advantages, Applications, and Extensions. *Annual Review of Psychology*, *67*, 641–66.

Gluth, S., Rieskamp, J., & Büchel, C. (2013). Classic EEG motor potentials track the emergence of value-based decisions. *NeuroImage*, *79*, 394–403.

Gold, J. I., & Shadlen, M. N. (2000). Representation of a perceptual decision in developing oculomotor commands. *Nature*, *404*, 390–94.

Gold, J. I., & Shadlen, M. N. (2003). The influence of behavioral context on the representation of a perceptual decision in developing oculomotor commands. *Journal of Neuroscience*, *23*, 632-51.

Hadar, A., Makris, S., & Yarrow, K. (2012). The truth-telling motor cortex: Response competition in M1 discloses deceptive behaviour. *Biological Psychology*, *89*, 495–502.

Hadar, A., Rowe, P., Di Costa, S., Jones, A., & Yarrow, K. (2016). Motor-evoked potentials reveal a motor-cortical readout of evidence accumulation for sensorimotor decisions. *Psychophysiology*, *15*, 49.

Hanks, T. D., & Summerfield, C. (2017). Perceptual Decision Making in Rodents, Monkeys, and Humans. *Neuron*, *93*, 15–31.

Heathcote, A., Brown, S., & Mewhort, D. J. K. (2002). Quantile maximum likelihood estimation of response time distributions. *Psychonomic Bulletin and Review*, *9*, 1–31.

Hick, W. E. (1952). On the rate of gain of information. *Quarterly Journal of Experimental Psychology*, *4*, 11–26.

Ho, T. C., Brown, S., & Serences, J. T. (2009). Domain General Mechanisms of Perceptual Decision

Making in Human Cortex. *Journal of Neuroscience*, *29*, 8675–87.

Kelly, S. P., & O'Connell, R. G. (2013). Internal and external influences on the rate of sensory evidence accumulation in the human brain. *Journal of Neuroscience*, *33*, 19434–41.

Kiers, L., Fernando, B., & Tomkins, D. (1997). Facilitatory effect of thinking about movement on magnetic motor-evoked potentials. *Electroencephalography and Clinical Neurophysiology - Electromyography and Motor Control*, *105*, 262–68.

Klein-Flugge, M. C., & Bestmann, S. (2012). Time-Dependent Changes in Human Corticospinal Excitability Reveal Value-Based Competition for Action during Decision Processing. *Journal of Neuroscience*, *32*, 8373–82.

Klein-Flügge, M., Nobbs, D., Pitcher, J., & Bestmann, S. (2013). Variability of human corticospinal excitability tracks the state of action preparation. *Journal of Neuroscience*, *33*, 5564–72.

Kleiner, M., Brainard, D. H., Pelli, D. G., Broussard, C., Wolf, T., & Niehorster, D. (2007). What's new in Psychtoolbox-3? *Perception*, *36*.

Konstantinos, T., Pfeffer, T., Jentgens, P., & Donner, T. H. (2015). Action planning and the timescale of evidence accumulation. *PLoS ONE*, *10*, 1–21.

Lee, K.-M., & Keller, E. L. (2008). Neural Activity in the Frontal Eye Fields Modulated by the Number of Alternatives in Target Choice. *Journal of Neuroscience*, *28*, 2242–51.

Li, X., & Aruin, A. (2005). Muscle activity onset time detection using teager-kaiser energy operator. *Conference Proceedings: IEEE 7*, 7549–52.

Li, X., Zhou, P., & Aruin, A. S. (2007). Teager-kaiser energy operation of surface EMG improves muscle activity onset detection. *Annals of Biomedical Engineering*, *35*, 1532–8.

McMillen, T., & Holmes, P. (2006). The dynamics of choice among multiple alternatives. *Journal of Mathematical Psychology*, *50*, 30–57.

Michelet, T., Duncan, G. H., & Cisek, P. (2010). Response Competition in the Primary Motor Cortex: Corticospinal Excitability Reflects Response Replacement During Simple Decisions. *Journal of Neurophysiology*, *104*, 119–27.

Mulder, M. J., van Maanen, L., & Forstmann, B. U. (2014). Perceptual decision neurosciences - a

model-based review. *Neuroscience*, *277*, 872–84.

O'Connell, R. G., Dockree, P. M., & Kelly, S. P. (2012). A supramodal accumulation-to-bound signal that determines perceptual decisions in humans. *Nature Neuroscience*, *15*, 1729–35.

Paré, M., & Wurtz, R. H. (2001). Progression in neuronal processing for saccadic eye movements from parietal cortex area LIP to superiorcolliculus. *Journal of Neurophysiology*, *85*, 2545–62.

Pelli, D. G. (1997). The VideoToolbox software for visual psychophysics: transforming numbers into movies. *Spatial Vision*.

Price, K. V., Storn, R. M., & Jouni, L. A. (2005). *Differential Evolution: A Practical Approach to Global Optimization*. Heidelberg: Springer Berlin Heidelberg.

Purcell, B. A., & Palmeri, T. J. (2017). Relating accumulator model parameters and neural dynamics. *Journal of Mathematical Psychology*, *76*, 156–171.

Ratcliff, R., & McKoon, G. (2008). The diffusion decision model: theory and data for two-choice decision tasks. *Neural Computation*, *20*, 873–922.

Ratcliff, R., & Rouder, J. N. (1998). Modeling Response Times for Two-Choice Decisions. *Psychological Science*, *9*(5), 347–56.

Roe, R. M., Busemeyer, J. R., & Townsend, J. T. (2001). Multialternative decision field theory: A dynamic connectionst model of decision making. *Psychological Review*, *108*, 370–92.

Roitman, J. D., & Shadlen, M. N. (2002). Response of neurons in the lateral intraparietal area during a combined visual discrimination reaction time task. *Journal of Neuroscience*, *22*, 9475–89.

Schwarz, G. E. (1978). Estimating the dimension of a model. *Annals of Statistics*, *6*, 461–64.

Shadlen, M. N., & Newsome, W. T. (2001). Neural Basis of a Perceptual Decision in the Parietal Cortex (Area LIP) of the Rhesus Monkey. *Journal of Neurophysiology*, *86*, 1916–36.

Selen, L. P. J., Shadlen, M. N., & Wolpert, D. M. (2012). Deliberation in the motor system: Reflex gains track evolving evidence leading to a decision. *Journal of Neuroscience*, *32*, 2276–86.

Servant, M., White, C., Montagnini, A., & Burle, B. (2015). Using covert response activation to test latent assumptions of formal decision-making models in humans. *Journal of Neuroscience*, *35*, 10371-85.

Servant, M., White, C., Montagnini, A., & Burle, B. (2016). Linking theoretical decision-making mechanisms in the simon task with electrophysiological data: A model-based neuroscience study in humans. *Journal of Cognitive Neuroscience, 28*, 1501-1521.

Siegel, M., Engel, A. K., & Donner, T. H. (2011). Cortical Network Dynamics of Perceptual Decision-Making in the Human Brain. *Frontiers in Human Neuroscience*, *5*, 1–12.

Smith, P. L., & Ratcliff, R. (2004). Psychology and neurobiology of simple decisions. *Trends in Neurosciences*, *27*, 161–168.

Solnik, S., Rider, P., Steinweg, K., Devita, P., & Hortobágyi, T. (2010). Teager-Kaiser energy operator signal conditioning improves EMG onset detection. *European Journal of Applied Physiology*, *110*, 489–498.

Spieser, L., Kohl, C., Forster, B., Bestmann, S., & Yarrow, K. (2018). Neurodynamic Evidence Supports a Forced- Excursion Model of Decision-Making under Speed/Accuracy Instructions. *ENeuro*, 0159-18.

Teodorescu, A. R., & Usher, M. (2013). Disentangling decision models: from independence to competition. *Psychological Review*, *120*, 1–38.

Thura, D., Beauregard-Racine, J., Fradet, C.-W., & Cisek, P. (2012). Decision making by urgency gating: theory and experimental support. *Journal of Neurophysiology*, *108*, 2912–2930.

Thura, D., & Cisek, P. (2016). Modulation of Premotor and Primary Motor Cortical Activity during Volitional Adjustments of Speed-Accuracy Trade-Offs. *Journal of Neuroscience*, *36*, 938–956.

Tsetsos, K., Usher, M., & Chater, N. (2010). Preference reversal in multiattribute choice. *Psychological Review*, *117*, 1275–1291.

Tsetsos, K., Usher, M., & McClelland, J. L. (2011). Testing multi-alternative decision models with non-stationary evidence. *Frontiers in Neuroscience*, *5*, 1–18.

Usher, M., & McClelland, J. L. (2001). The time course of perceptual choice: The leaky, competing accumulator model. *Psychological Review*, *108*, 550–592.

Wyart, V., Myers, N. E., & Summerfield, C. (2015). Neural Mechanisms of Human Perceptual Choice Under Focused and Divided Attention. *Journal of Neuroscience*, *35*, 3485–3498.

Tables

Table 1: Model comparison: BIC, AIC and likelihood values for each model. Model 1 has the lowest (best) BIC and AIC values (best BIC and AIC values in bold).

Model	Number of parameters	AIC	BIC	Likelihood	Parameters
Model 1	10	**141,600**	**141,684**	*-70,790*	$v_{easy\text{-}correct}$, $v_{easy\text{-}incorrect}$, $v_{hard\text{-}correct}$, $v_{hard\text{-}incorrect}$, $z_{two\text{-}choice\text{-}cued}$, k, β_{adj}, β_{opp}, σ^2, T_{er}
Model 2	10	142,172	142,256	*-71,076*	$v_{easy\text{-}correct}$, $v_{easy\text{-}incorrect}$, $v_{hard\text{-}correct}$, $v_{hard\text{-}incorrect}$, $z_{two\text{-}choice\text{-}cued}$, k, β_{adj}, β_{opp}, σ^2, T_{er}
Model 3	13	144,859	144,968	*-72,410*	$v_{easy\text{-}four\text{-}correct}$, $v_{easy\text{-}four\text{-}incorrect}$, $v_{easy\text{-}two\text{-}correct}$, $v_{easy\text{-}two\text{-}incorrect}$, $v_{hard\text{-}four\text{-}correct}$, $v_{hard\text{-}four\text{-}incorrect}$, $v_{hard\text{-}two\text{-}correct}$, $v_{hard\text{-}two\text{-}incorrect}$, k, β_{adj}, β_{opp}, σ^2, T_{er}

Table 2: Estimated parameter values for the chosen model (Model 1): note that the response boundary A was set to 1 as a scaling parameter, and that the starting-point z was set to 0 for four-choice trials.

Model 1: LCA Parameters			
Leakage (k)			0.000029
Boundary (A)			1
Non-decision time (T_{er})			0.2994
Diffusion constant (σ^2)			0.4863
Inhibition (β)		β_{adj}	0.000022
		β_{opp}	0.0408
Starting point (z)		two-choice (cued)	0.2355
		four-choice/ two-choice (uncued)	0
Accumulation rate (v)	easy	correct	1.3199
		incorrect	0.2321
	hard	correct	1.1781
		incorrect	0.3413

Figure Captions

Figure 1:

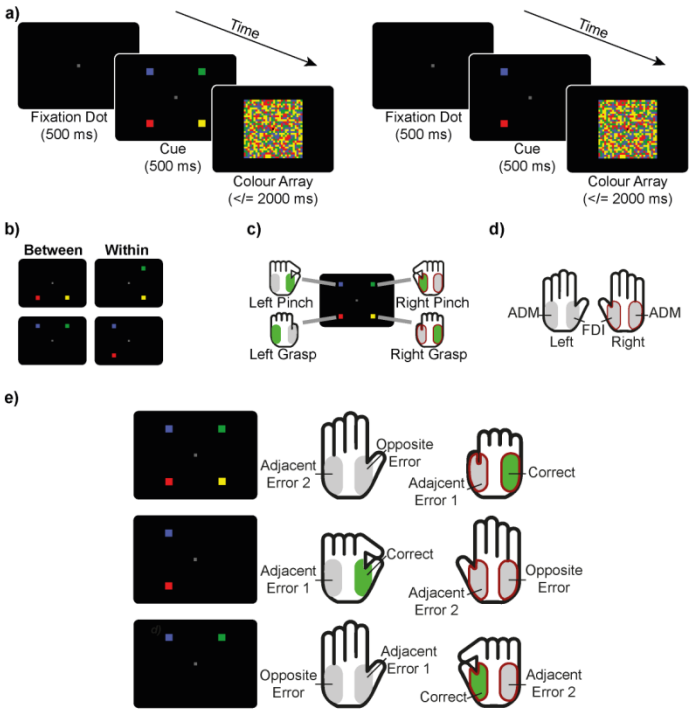

Trial Procedure: a) colour discrimination task; participants have to indicate which of the pre-cued colours is the most prevalent on the colour array. Left: four-choice trial: all possible cues were displayed. Right: two-choice trial: only two of the possible cues were shown. b) all possible two-choice combinations. In 'within' trials, both possible responses were on the same hand, while in 'between' trials, the two possible responses were on different hands but using the same response (pinch/grasp). c) each cue/colour was associated with a specific response: the top right cue (here: green) was associated with a right-hand 'pinch' response, the top left cue (here: blue) with a left-hand 'pinch' response, the

bottom right cue (here: yellow) with a right-hand ‘grasp’ response, and the bottom left cue (here: red) with a left-hand ‘grasp’ response. Colour-response mappings were randomised across participants while the cue location-response mapping remained the same. d) each hand performed pinch and grasp responses, recruiting the first dorsal interosseous (FDI) and abductor digiti minimi (ADM) muscles respectively. Muscles associated with correct responses are shown in green, while others are displayed in grey (see c & e). MEPs were only recorded from right-hand muscles (indicated by dark red border). e) response categorisation. In each trial, right-hand MEPs are associated with two of the response categories. Activation of all categories is probed across trials, as the position of the correct response varied randomly. Top panel: four-choice trial in which the stimulus array (not shown) instructs a right grasp response. The incorrect response on the same hand is labelled ‘Adjacent Error 1’, and the responses on the other hand are labelled ‘Adjacent Error 2’ (homologous to correct response) and ‘Opposite Error’ (non-homologous to correct response). Middle panel: Two-choice ‘within’ trial, here involving a choice between left-hand responses. If the left pinch response is correct, the incorrect but cued response (here left grasp) is classed as ‘Adjacent Error 1’, the response homologous to the correct one on the other hand is labelled ‘Adjacent Error 2’ and the opposite response is labelled ‘Opposite Error’. Bottom panel: Two-choice ‘between’ trial, involving selecting among left or right pinch responses. Here the right pinch is correct and the left pinch, which is cued but incorrect, is ‘Adjacent Error 1’. The incorrect response on the same hand as the correct response is labelled ‘Adjacent Error 2’, and the anatomically opposite response is called ‘Opposite Error’.

Figure 2:

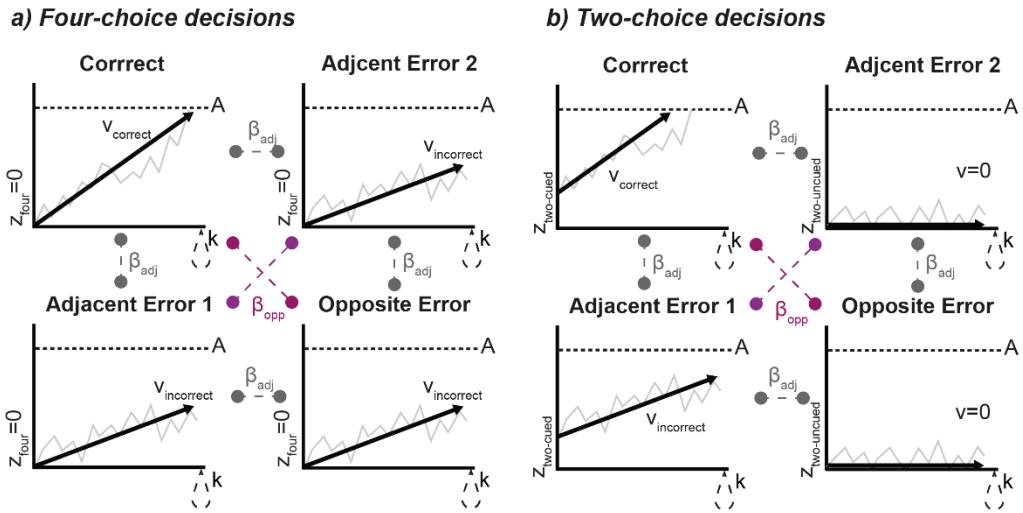

LCA model: a) Four-choice decisions. Four accumulators race towards boundary A (fixed to 1). Each accumulator starts at a starting point $z_{four\text{-}choice}$ (fixed to 0). The accumulator associated with the correct alternative increases at a mean rate $v_{correct}$ while other accumulators increase at mean rate $v_{incorrect}$. Accumulators are affected by leakage over time (k, black, dashed). Two inhibition parameters define the inhibition between accumulators. 'Opposite' accumulators (i.e., representing non-homologuous responses on different hands) inhibit each other with a strength of β_{opp} (purple, dashed). All others (i.e., all adjacent) accumulators inhibit each other with a strength of β_{adj} (grey, dashed). b) Two-choice decisions. Here, the two uncued responses ('Adjacent Error 2' & 'Opposite Error') accumulate only noise (mean rate of 0). The starting points of the accumulators associated with the two cued responses, defined by $z_{two\text{-}choice\text{-}cued}$, are yoked as a (positively signed) free parameter.

Figure 3:

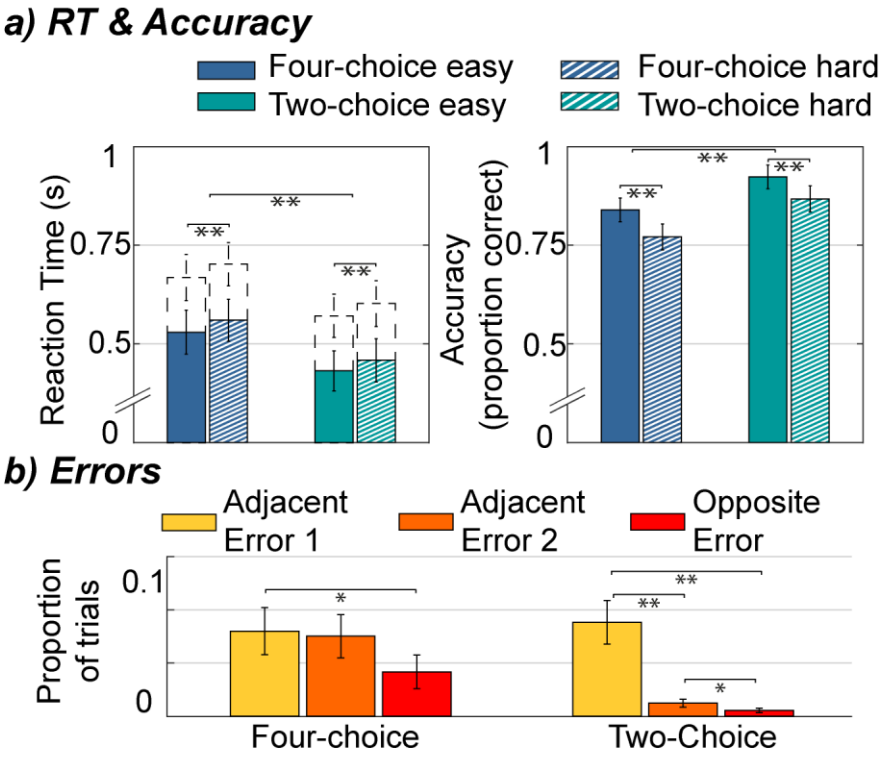

Behavioural results: a) mean reaction times (left) and accuracy (right) by condition. EMG RTs are shown as filled bars; button RTs are indicated using dashed lines. b) Proportion of errors per error category for four-choice (left) and two-choice (right) trials. Error bars indicate 95% confidence intervals. * indicates $p < .05$, ** indicates $p < .001$.

Figure 4:

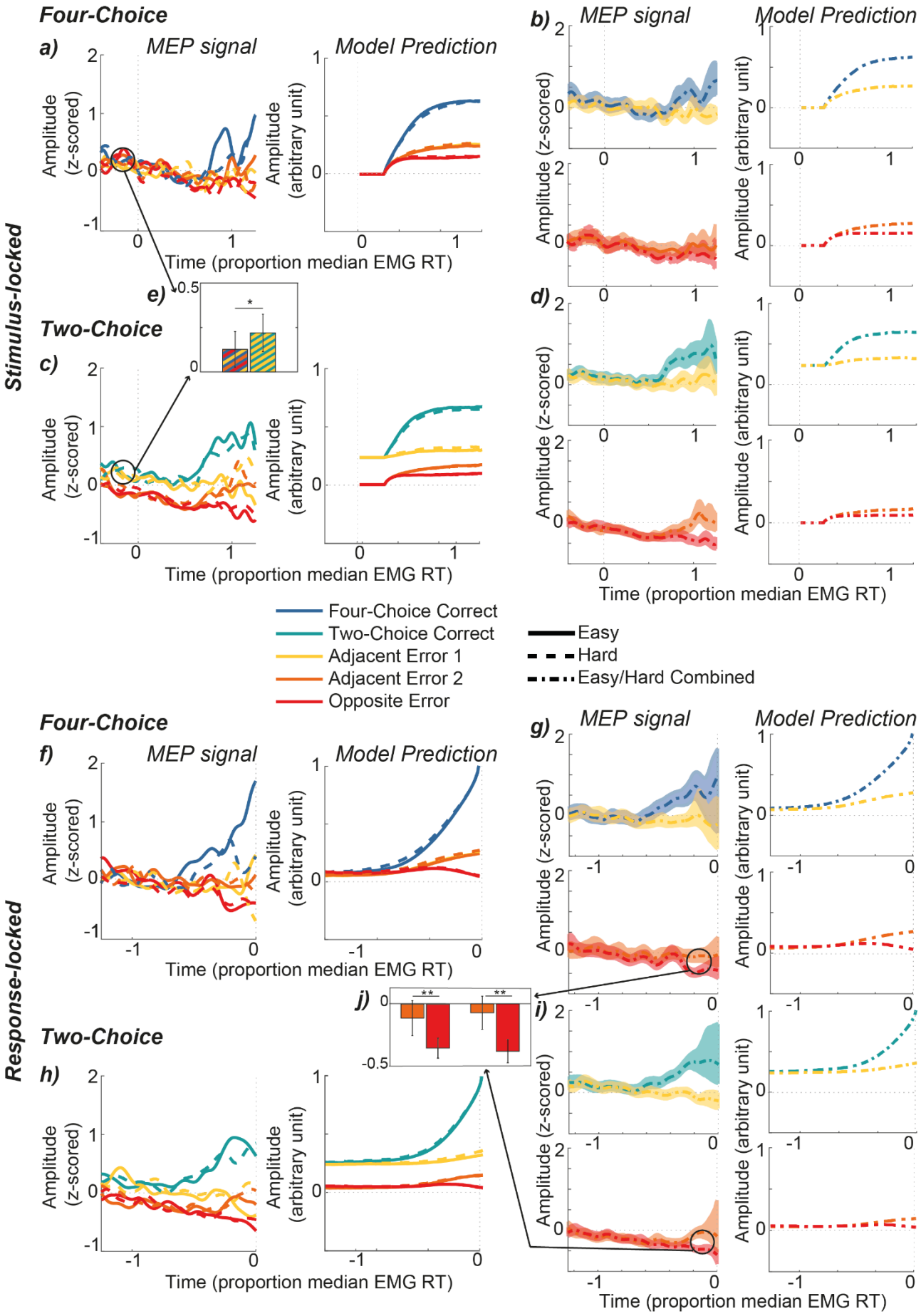
Four-Choice
a)
MEP signal
Model Prediction
Amplitude (z-scored)
Amplitude (arbitrary unit)
Time (proportion median EMG RT)
b)
MEP signal
Model Prediction
Amplitude (z-scored)
Amplitude (arbitrary unit)
Time (proportion median EMG RT)
Stimulus-locked
e)
Two-Choice
c)
d)
Four-Choice Correct
Two-Choice Correct
Adjacent Error 1
Adjacent Error 2
Opposite Error
Easy
Hard
Easy/Hard Combined
Four-Choice
f)
MEP signal
Model Prediction
g)
MEP signal
Model Prediction
Response-locked
j)
Two-Choice
h)
i)

MEP results and Model Predictions: Smoothed MEP signals (*'MEP signal'* columns) and LCA predictions ('*Model Prediction*' columns) for both stimulus-locked (top: a - e) and response-locked (bottom: f - j) signals. Shaded areas and error bars indicate 95% CI, * $p < .05$, ** <.001.

a/f) MEP signals (left) and model predictions (right) associated with four-choice trials. In each panel, signals from easy (solid lines) and hard (dashed lines), as well as each correct/error category ('Correct', 'Adjacent Error 1', Adjacent 'Error 2', 'Opposite Error') are displayed separately.

b/g) Four-choice MEP signals (left) and model predictions (right) collapsed over easy and hard trials.

c/h) MEP signals (left) and model predictions (right) associated with two-choice trials. Data are divided as per panels a/f.

d/i) Two-choice MEP signals (left) and model predictions (right) collapsed over easy and hard trials.

e) Top inset panel shows amplitude differences between four-choice (left bar) and cued two-choice (right bar) baseline activity (note that, unlike the rest of the figure, this bar chart contained data from both correct and incorrect trials).

j) Bottom inset panel shows amplitude differences between terminal 'Adjacent Error2' and 'Opposite Error' data in both four-choice (left) and two-choice (right) trials.

Figure 5:

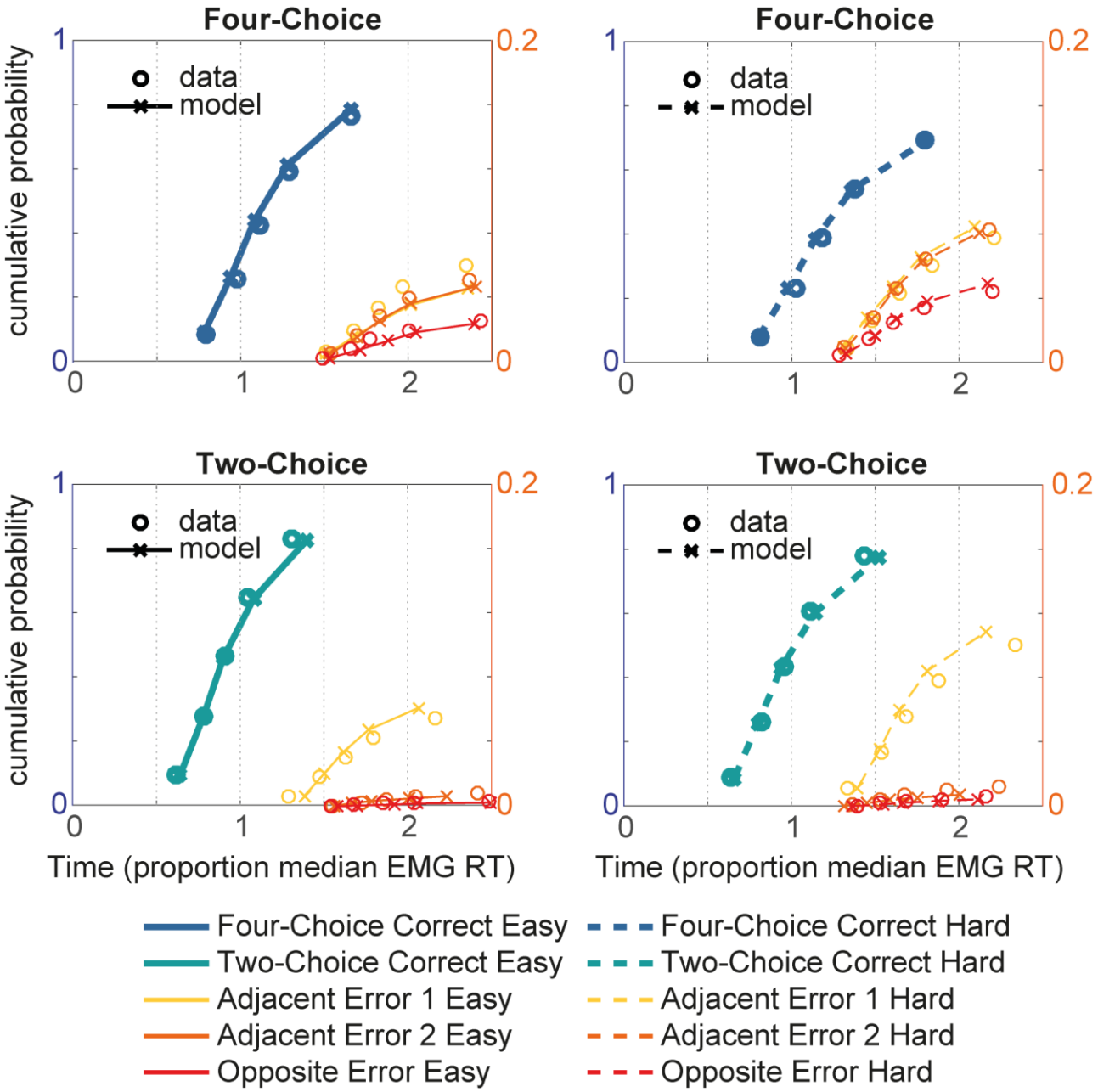

Model fit: quantiles estimated from behavioural data (circles) and LCA simulations (crosses and lines) for four-choice (top) and two-choice (bottom) decisions. Note that incorrect trials (yellow/orange/red, right-hand ordinate) are shown on a magnified scale compared to correct trials (blue, left-hand ordinate).